Structural aspects of B_2O_3-substituted $(PbO)_{0.5}(SiO_2)_{0.5}$ glasses

2002 J. Phys.: Condens. Matter 14 6553

(http://iopscience.iop.org/0953-8984/14/25/322)

INSTITUTE OF PHYSICS PUBLISHING JOURNAL OF PHYSICS: CONDENSED MATTER

J. Phys.: Condens. Matter **14** (2002) 6553–6565 PII: S0953-8984(02)34203-6

Structural aspects of B_2O_3-substituted $(PbO)_{0.5}(SiO_2)_{0.5}$ glasses

V Sudarsan[1], **V K Shrikhande**[2], **G P Kothiyal**[2] **and S K Kulshreshtha**[1,3]

[1] Novel Materials and Structural Chemistry Division, Bhabha Atomic Research Centre, Mumbai-400 085, India

[2] Technical Physics and Prototype Engineering Division, Bhabha Atomic Research Centre, Mumbai-400 085, India

E-mail: kulshres@magnum.barc.ernet.in

Received 25 February 2002, in final form 21 May 2002
Published 14 June 2002
Online at stacks.iop.org/JPhysCM/14/6553

Abstract

Lead borosilicate glasses having general formulae $(PbO)_{0.5-x}(SiO_2)_{0.5}(B_2O_3)_x$ with $0.0 \leqslant x \leqslant 0.4$ and $(PbO)_{0.5}(SiO_2)_{0.5-y}(B_2O_3)_y$ with $0.0 \leqslant y \leqslant 0.5$ have been prepared by a conventional melt–quench method and characterized by ^{29}Si, ^{11}B magic angle spinning (MAS) NMR techniques and infrared spectroscopy, as regards their structural features. From ^{29}Si NMR results, it has been inferred that with increasing concentration of boron oxide, $(PbO)_{0.5-x}(SiO_2)_{0.5}(B_2O_3)_x$ glasses exhibit a systematic increase in the number of Q^4 structural units of Si at the expense of Q^2 structural units, along with the formation of Si–O–B linkages. On the other hand, for $(PbO)_{0.5}(SiO_2)_{0.5-y}(B_2O_3)_y$ glasses, there is no direct interaction between SiO_2 and B_2O_3 in the glass network, as revealed by the ^{29}Si MAS NMR studies. Boron exists in both trigonal and tetrahedral configurations for these two series of glasses and for the $(PbO)_{0.5}(SiO_2)_{0.5-y}(B_2O_3)_y$ series of glasses; the relative concentration of these two structural units remains almost constant with increasing B_2O_3 concentration. In contrast, for $(PbO)_{0.5-x}(SiO_2)_{0.5}(B_2O_3)_x$ glasses, there is a slight increase in the number of BO_3 structural units above $x = 0.2$, as there is a competition between SiO_2 and B_2O_3 for interaction with Pb^{2+}, thereby leading to the formation of BO_3 structural units. For both series of glasses, the thermal expansion coefficient is found to decrease with increasing B_2O_3 concentration, the effect being more pronounced for the $(PbO)_{0.5-x}(SiO_2)_{0.5}(B_2O_3)_x$ series of glasses due to the increased concentration of Q^4 structural units of silicon and better cross-linking as a result of the formation of Si–O–B-type linkages.

[3] Author to whom any correspondence should be addressed.

1. Introduction

$PbO–SiO_2$-based glasses are technologically important and have potential applications in making ultrasonic delay cables, electron multipliers, TV picture tubes, glass-to-metal seals etc [1–3]. The binary $PbO–SiO_2$ system has been thoroughly studied as regards its structural aspects by various authors [4–7]. Wang and Zhang [4] suggested, on the basis of XPS studies of these glasses, that addition of PbO up to 40 mol% to silica results in the modification of the extended silica network and further addition results in the formation of a $(PbO_4)_n$ network interconnected by discrete silica structural configurations. Fayon *et al* [6] suggested, on the basis of their ^{207}Pb NMR and Pb L_{III}-edge EXAFS studies, the existence of PbO_4 and PbO_3 types of structural configuration in these glasses and their relative amounts changed with change in the SiO_2-to-PbO mole ratio. The same authors, in an earlier study, identified different types of silicon structural configuration present in these glasses by the ^{29}Si MAS NMR technique [7]. From these studies it has been inferred that PbO can act both as a network former and as a network modifier in lead silicate glasses, depending upon its relative concentration. It is of interest to study this behaviour of PbO, when another network-forming oxide, such as B_2O_3, is present along with the binary lead silicate system. Addition of B_2O_3 to $PbO–SiO_2$ glasses is expected to modify its physico-chemical properties such as mechanical strength, dielectric constant and refractive index, as boron can exist both in trigonal and in tetrahedral configurations, depending upon the PbO-to-B_2O_3 and SiO_2-to-B_2O_3 mole ratios. The structural aspects of $PbO–B_2O_3–SiO_2$ glasses have been studied by Kim *et al* [8] using the ^{11}B and ^{207}Pb static NMR technique and it was suggested that Pb^{2+} is evenly shared between B–O and Si–O networks and plays an important role in deciding the relative concentration of BO_4 and BO_3 structural configurations. The authors did not investigate the ^{29}Si NMR spectra of these glasses, which can provide very useful information regarding the different configurations of silicon as well as the existence of different types of chemical interaction existing between the constituent oxides of these glasses. Extensive studies have been reported for borosilicate glasses containing alkali oxides using ^{11}B, ^{29}Si MAS NMR and Raman spectroscopic techniques and, based on these results, a composition-dependent interaction of alkali metal ions with the borate and silicate network has been suggested for these glasses [9–11]. PbO is known to behave like alkali metal oxides and thus it is of interest to study the $PbO–SiO_2–B_2O_3$ glass system with a view to achieving an understanding of the effect of PbO addition to the borosilicate network present in these glasses.

In general, the physical properties of the glasses such as the thermal expansion coefficient and the glass transition temperature are expected to depend on the nature of the linkages present in the glass network [12, 13]. For example, Klyuev and Pevzner [12] have studied the variation of the glass transition temperature and thermal expansion coefficient as a function of the composition of boroaluminate glasses having Al_2O_3/BaO ratios of 1.0 and 0.5 and they tried to correlate the variation of the glass transition temperature and the structural thermal expansion coefficient with the concentration of BO_3 structural units. On the basis of these studies, it has been reported that for concentrations of BO_3 up to $\approx$0.70 there was no appreciable variation in the glass transition temperature or the structural thermal expansion coefficient, but for even higher concentrations of BO_3 there was a sharp decrease in the value of the glass transition temperature and a significant increase in the value of the thermal expansion coefficient. In an another study of fluorophosphate glasses, Karmakar *et al* [13] have shown that the glass transition temperature and absorption coefficient at 2170 cm^{-1}, which arises due to the overtone of $2\nu_{ss}$(OPO) and/or the combination (ν_{as}(OPO) + ν_{as}(POP)) which are the fundamental vibrations of glass-forming PO_4 tetrahedra, showed a similar dependence on the contents of fluoride ions in these glasses. On the basis of the statistical analysis of the observed results, these authors have suggested that the values of the glass transition temperature and the thermal expansion coefficient are correlated with the absorption coefficient at 2170 cm^{-1}. In an earlier study [14], preliminary results on the variation of the thermal expansion and glass transition temperature for $PbO–SiO_2–B_2O_3$ glasses as a function of B_2O_3 concentration were reported and a qualitative correlation between the values of the glass transition temperature and the concentration of Q^4 structural units, determined by ^{29}Si MAS NMR spectroscopy, was observed for $(PbO)_{0.5-x}(SiO_2)_{0.5}(B_2O_3)_x$ glasses. Furthermore, the values of the thermal expansion coefficient for these glasses showed a systematic decrease with increase in B_2O_3 concentration.

In the present communication, results of the detailed study of the structural aspects of two series of glasses, namely $(PbO)_{0.5-x}(SiO_2)_{0.5}(B_2O_3)_x$ and $(PbO)_{0.5}(SiO_2)_{0.5-y}(B_2O_3)_y$, are reported; the study used both ^{11}B and ^{29}Si as probe nuclei, for the composition range over which glass formation occurs [15], with a view to correlating the values of the thermal expansion coefficient and glass transition temperature with the structural features of these glasses.

2. Experimental details

Two series of glasses having general formulae $(PbO)_{0.5-x}(SiO_2)_{0.5}(B_2O_3)_x$ and $(PbO)_{0.5}(SiO_2)_{0.5-y}(B_2O_3)_y$ with $0.0 \leqslant x \leqslant 0.4$ and $0.0 \leqslant y \leqslant 0.5$ were prepared by melting a well ground mixture containing stoichiometric quantities of PbO, SiO_2 and H_3BO_3 in platinum crucibles at about 850–900 °C, poured and quenched in between brass plates. Powder x-ray diffraction studies were carried out using a Philips PW1710 x-ray diffractometer to confirm the glass formation in these samples. ^{29}Si and ^{11}B MAS NMR patterns were recorded using a Bruker Avance DPX 300 machine with basic frequencies of 59.62 and 96.29 MHz respectively. Samples were spun at 5 kHz for the MAS NMR experiments. Typical 90° pulse durations for the ^{29}Si and ^{11}B NMR experiments were 4.5 and 2.09 μs, respectively. A relaxation delay of 5 s was employed for both the nuclei. ^{29}Si MAS NMR patterns were deconvoluted into individual Gaussian peaks arising due to different types of silicon structural configuration, using a least-squares fitting procedure. Further, it has been observed that for all the patterns, deconvolution into three peaks resulted in optimum fitting as revealed by the minimum value of χ^2. The observed ^{11}B MAS NMR patterns have been corrected for the contribution due to the BN present in the Bruker MAS NMR probe. ^{11}B MAS NMR patterns were qualitatively analysed to estimate the relative abundance of trigonal and tetrahedral boron structural units. These spectra could not be deconvoluted into component spectra due to the quadrupolar nature of the ^{11}B nucleus and the varying values of electric field gradient felt by ^{11}B nuclei in the glass structure.

Average thermal expansion coefficients were measured using a dilatometer (model TMA-92, M/s. Setaram, France). The sample (10 mm in diameter and 5–10 mm in height) was mounted on the quartz sample holder, located inside the measurement chamber. The chamber was evacuated to 10^{-3} mbar and then flushed with high-purity argon. The argon flow rate was maintained at 40 l min^{-1} and the sample was heated at 10 K min^{-1} under a constant load of 5 g, for the thermal expansion measurements. The average value of the thermal expansion coefficient was estimated by measuring the change in the length of the sample between 50 and 300 °C. The glass transition temperature was determined from the intersection of the linear portions of this curve, which were extrapolated from the temperature regions below and above the glass transition temperature.

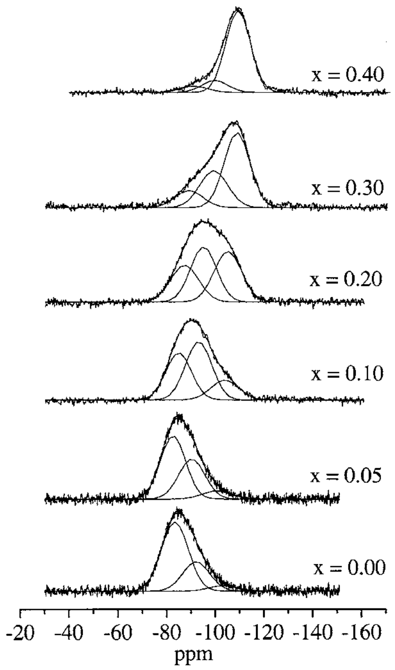

Figure 1. Deconvoluted ^{29}Si MAS NMR patterns of $(PbO)_{0.5-x}(SiO_2)_{0.5}(B_2O_3)_x$ glasses for $0.0 \leqslant x \leqslant 0.4$.

3. Results

Powder x-ray diffraction patterns of all the samples were recorded by using Cu Kα x-rays and showed two very broad peaks characteristic of glass structure and positioned over the regions 25°–30° and 40°–50° (2θ values).

3.1. ^{29}*Si MAS NMR studies*

Figure 1 shows the ^{29}Si MAS NMR patterns of $(PbO)_{0.5-x}(SiO_2)_{0.5}(B_2O_3)_x$ glasses with $0.0 \leqslant x \leqslant 0.4$ along with their deconvoluted patterns. For the binary $(PbO)_{0.5}(SiO_2)_{0.5}$ glass composition, the NMR pattern has been found to consist of three peaks placed at around -102.9, -95.1 and -83.4 ppm (with respect to tetramethylsilane) which are characteristic of Q^4, Q^3 and Q^2 structural configurations of silicon respectively (here Q^n, with $1 \leqslant n \leqslant 4$, represents the silicon structural configuration with n the number of bridging oxygen atoms around it); these values are in good agreement with the results reported by Fayon *et al* [7]. From this figure it is clear that as PbO is systematically replaced by B_2O_3, the relative intensity of the Q^4 configuration increases at the expense of the Q^2 structural configuration. The intensity of the Q^3 structural configuration shows a slight increase initially and then decreases. Figure 2 shows the ^{29}Si MAS NMR patterns of $(PbO)_{0.5}(SiO_2)_{0.5-y}(B_2O_3)_y$ glasses where a proportion of the SiO_2 has been replaced by B_2O_3, for $0.0 \leqslant y \leqslant 0.3$, along with their deconvoluted components. All the patterns were found to contain mainly Q^3 and Q^2 structural configurations along with small amounts of Q^4 structural configurations. The relative intensity of different structural configurations of silicon and their chemical shift values for both $(PbO)_{0.5-x}(SiO_2)_{0.5}(B_2O_3)_x$ and $(PbO)_{0.5}(SiO_2)_{0.5-y}(B_2O_3)_y$ glasses are plotted in figures 3(a) and (b), respectively, as a func-

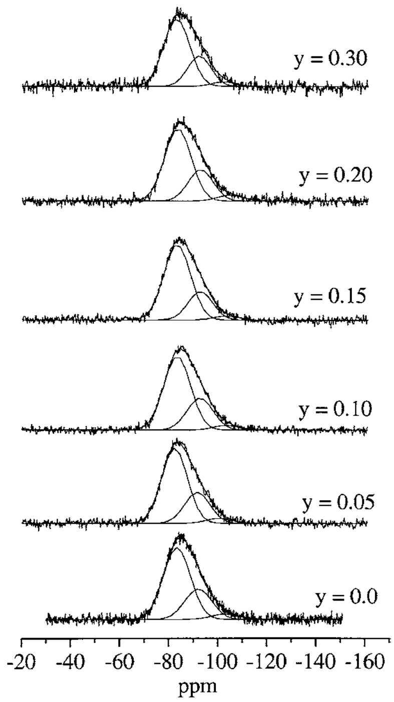

Figure 2. Deconvoluted ^{29}Si MAS NMR patterns of $(PbO)_{0.5}(SiO_2)_{0.5-y}(B_2O_3)_y$ glasses with $0.0 \leqslant y \leqslant 0.3$.

tion of B_2O_3 content. It may be specifically mentioned that for none of these compositions have Q^1 and Q^0 structural configurations been observed. For $(PbO)_{0.5-x}(SiO_2)_{0.5}(B_2O_3)_x$ glasses, the chemical shift values, for Q^4, Q^3 and Q^2 structural configurations of silicon, have been found to show systematic decrease with increase in the B_2O_3 content (see figure 3(a)). In contrast, the relative amounts of different Q^n structural units and their chemical shift values remained almost unaffected for $(PbO)_{0.5}(SiO_2)_{0.5-y}(B_2O_3)_y$ glasses, as can be seen from figure 3(b).

3.2. ^{11}B MAS NMR studies

Figure 4 shows ^{11}B MAS NMR patterns of $(PbO)_{0.5-x}(SiO_2)_{0.5}(B_2O_3)_x$ glasses with $0.1 \leqslant x \leqslant 0.4$. These patterns are each composed of a sharp peak superimposed over a broad and asymmetric peak. The spinning sidebands corresponding to these two patterns were also observed. These two patterns correspond to the tetrahedral and trigonal configurations of boron [9, 16]. Even though the line shapes for ^{11}B MAS NMR spectra are complex, qualitatively one can see that the relative intensity of the broad peak, below the sharp peak, increases systematically above $x = 0.2$.

Figure 5 shows ^{11}B MAS NMR patterns for the $(PbO)_{0.5}(SiO_2)_{0.5-y}(B_2O_3)_y$ series of glasses with $0.1 \leqslant y \leqslant 0.5$. The spectral features of these patterns have been found to be similar to those of $(PbO)_{0.5-x}(SiO_2)_{0.5}(B_2O_3)_x$ glasses with $0.1 \leqslant x \leqslant 0.4$. The relative intensity of the peaks corresponding to trigonal and tetrahedral configurations has been found to be almost constant, in spite of significant change in the B_2O_3 content, for these samples.

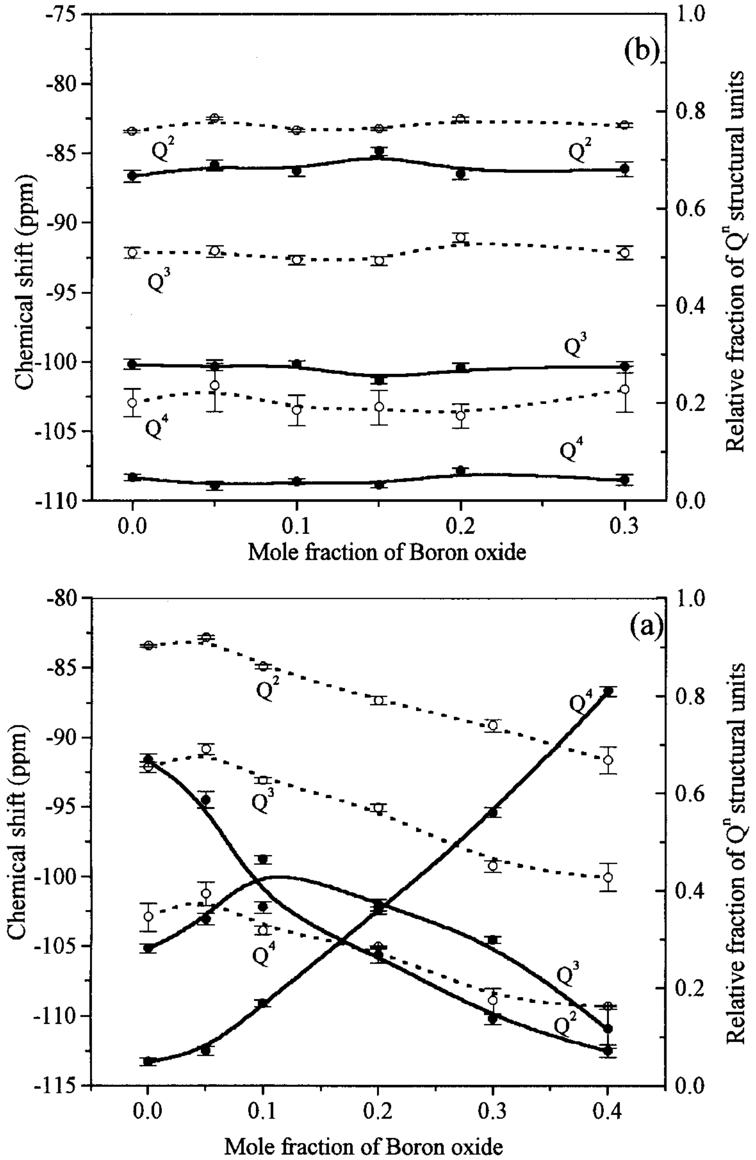

Figure 3. Variation of the relative intensity for different structural units of silicon (filled circles) and their chemical shift values (open circles) as a function of B_2O_3 concentration for (a) $(PbO)_{0.5-x}(SiO_2)_{0.5}(B_2O_3)_x$ glasses with $0.0 \leqslant x \leqslant 0.4$ and (b) $(PbO)_{0.5}(SiO_2)_{0.5-y}(B_2O_3)_y$ glasses with $0.0 \leqslant y \leqslant 0.3$.

3.3. Infrared studies

Figure 6 shows selected regions of the FTIR patterns for $(PbO)_{0.5}(SiO_2)_{0.5}$, $(PbO)_{0.5-x}(SiO_2)_{0.5}(B_2O_3)_x$ and $(PbO)_{0.5}(SiO_2)_{0.5-y}(B_2O_3)_y$ glasses with $x = y = 0.1$ and 0.3, over the region of 400–2500 cm^{-1}. The peak around 474 cm^{-1}, which corresponds to the bending mode of Si–O–Si linkages (figure 6(a)), is absent for $(PbO)_{0.5}(B_2O_3)_{0.5}$ glass (figure 6(b)). The absorption band at ~1315 cm^{-1} in figure 6(b) corresponds to the asymmetric

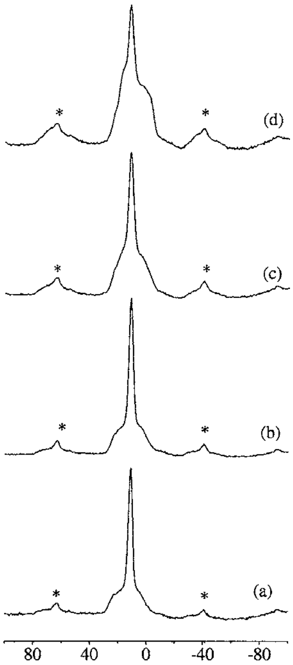

Figure 4. ^{11}B MAS NMR patterns of $(PbO)_{0.5-x}(SiO_2)_{0.5}(B_2O_3)_x$ glasses having x-values of (a) 0.1, (b) 0.2, (c) 0.3 and (d) 0.4. Peaks marked with asterisks correspond to spinning sidebands.

stretching vibrations of BO_3^{3-} structural units [17–19]. A comparison of this spectrum with the spectra of $(PbO)_{0.5-x}(SiO_2)_{0.5}(B_2O_3)_x$ samples (see figures 6(d) and (f)) reveals that the peak around 1315 cm^{-1} has shifted to higher wavenumbers, namely 1340 and 1380 cm^{-1}. On the other hand, the vibrational band due to BO_3^{3-} structural units remains almost unchanged in $(PbO)_{0.5}(SiO_2)_{0.5-y}(B_2O_3)_y$ glasses.

3.4. Thermal expansion and glass transition temperatures

Figures 7(a) and (b) show the variation of the average linear thermal expansion as a function of temperature for two representative samples, namely $(PbO)_{0.1}(SiO_2)_{0.5}(B_2O_3)_{0.4}$ and $(PbO)_{0.5}(SiO_2)_{0.1}(B_2O_3)_{0.4}$, respectively. From figure 7 it is clear that there is a significant difference in value of the glass transition temperature between these two samples. The slopes of the two curves over the temperature region of 50–300 °C have been found to be significantly different, the effect being more pronounced for $(PbO)_{0.5}(SiO_2)_{0.1}(B_2O_3)_{0.4}$ glass. The average thermal expansion coefficient defined as $[(\Delta L/L)/\Delta T]$ was evaluated over the temperature region where the variation of $\Delta L/L$ is linear. In the present study, the temperature region employed is from 50 to 300 °C. Figures 8(a) and (b) show the average values of the linear thermal expansion coefficient and the glass transition temperature as a function of B_2O_3 concentration for $(PbO)_{0.5-x}(SiO_2)_{0.5}(B_2O_3)_x$ glasses with $0.0 \leqslant x \leqslant 0.4$ and $(PbO)_{0.5}(SiO_2)_{0.5-y}(B_2O_3)_y$ glasses with $0.0 \leqslant y \leqslant 0.5$, respectively. For both series of glasses, the values of the linear thermal expansion coefficient show a systematic decrease with increasing concentration of B_2O_3, the effect being more pronounced when some of the PbO is replaced by B_2O_3. The average values of the linear thermal expansion coefficients for $(PbO)_{0.5}(SiO_2)_{0.5}$ and $(PbO)_{0.5}(B_2O_3)_{0.5}$ glasses are $\approx 11.1 \times 10^{-6}$ and 8.6×10^{-6} °C^{-1}, respectively. It is also observed that for both series, the values of the glass transition temperature

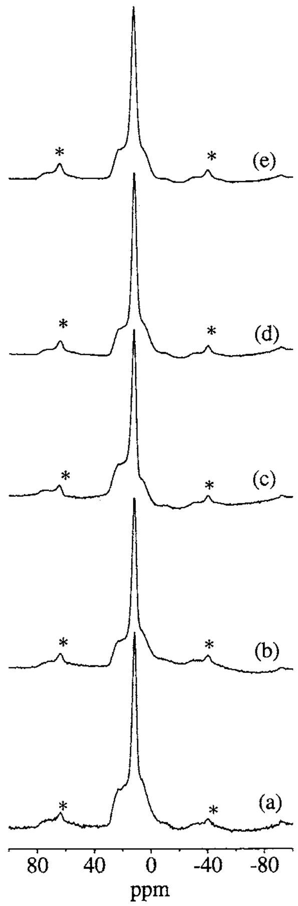

Figure 5. ^{11}B MAS NMR patterns of $(PbO)_{0.5}(SiO_2)_{0.5-y}(B_2O_3)_y$ glasses having y-values of (a) 0.1, (b) 0.15, (c) 0.2, (d) 0.3 and (e) 0.5. Peaks marked by asterisks correspond to spinning sidebands.

showed a systematic increase with increase in B_2O_3 concentration; however, the effect is more pronounced for $(PbO)_{0.5-x}(SiO_2)_{0.5}(B_2O_3)_x$ glasses. Figure 9 shows the variation of the values of the thermal expansion coefficient and glass transition temperature as a function of the mole fraction of Q^4 structural units of silicon for $(PbO)_{0.5-x}(SiO_2)_{0.5}(B_2O_3)_x$ glasses with $0.0 \leqslant x \leqslant 0.4$. This indicates that the variations of the thermal expansion coefficient and the glass transition temperature with respect to the concentration of Q^4 structural units are of opposite natures.

4. Discussion

From figure 3(a), it is clear that for the $(PbO)_{0.5-x}(SiO_2)_{0.5}(B_2O_3)_x$ system the relative intensity of different silicon structural configurations and their chemical shift values are found to depend on the B_2O_3 concentration. The systematic increase in the relative intensity of Q^4 structural units at the expense of Q^2 structural units can be understood in terms of the decreasing concentration of lead oxide and increasing concentration of network-former boron oxide, which will lead to an enhanced probability of formation of silicon atoms with the Q^4

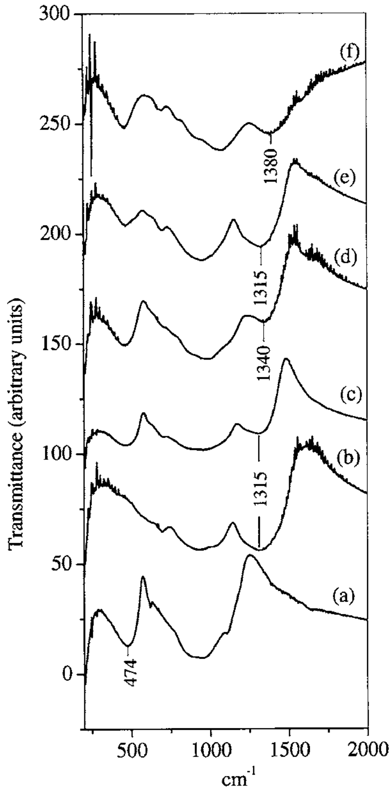

Figure 6. FTIR patterns of (a) $(PbO)_{0.5}(SiO_2)_{0.5}$, (b) $(PbO)_{0.5}(B_2O_3)_{0.5}$, (c) $(PbO)_{0.5}(SiO_2)_{0.4}(B_2O_3)_{0.1}$, (d) $(PbO)_{0.4}(SiO_2)_{0.5}(B_2O_3)_{0.1}$, (e) $(PbO)_{0.5}(SiO_2)_{0.2}(B_2O_3)_{0.3}$, (f) $(PbO)_{0.2}(SiO_2)_{0.5}(B_2O_3)_{0.3}$.

configuration. This also explains the initial increase in the concentration of Q^3 structural units and its subsequent decrease with increase in B_2O_3 concentration in these glasses. The systematic decrease in chemical shift values, observed for different structural configurations of silicon, as a result of B_2O_3 substitution in $(PbO)_{0.5-x}(SiO_2)_{0.5}(B_2O_3)_x$ glasses, arises due to the increased number of Si–O–B linkages formed at the expense of Si–O–Pb linkages, as the cationic field strength of B^{3+} is significantly higher than that of Pb^{2+} [20]. In contrast, for $(PbO)_{0.5}(SiO_2)_{0.5-y}(B_2O_3)_y$ glasses with $0.0 \leqslant y \leqslant 0.30$, the relative abundances of Q^4, Q^3 and Q^2 structural units and their chemical shift values remain almost constant for all the samples (see figure 3(b)), which indicates that there is no direct interaction between the borate and silicate structural units in these glasses. In such glasses the borate network may be indirectly interacting with the silicate network through Pb to form linkages of the type Si–O–(Pb–O)$_n$–B, where the boron atom may have only a negligible influence on the relative abundance of the different structural configurations of Si and their chemical shift values.

^{11}B MAS NMR patterns were found to be complex due to the highly overlapped sharp peak, characteristic of a tetrahedrally coordinated boron configuration, and broad peak, arising due to trigonally coordinated boron structural units. This is because, for half-integer quadrupolar nuclei such as boron, the central transition is affected by second-order quadrupolar interaction, which is significant for nuclei occupying non-cubic sites. Hence boron in a trigonal configuration gives rise to a broad peak even after magic angle spinning. In

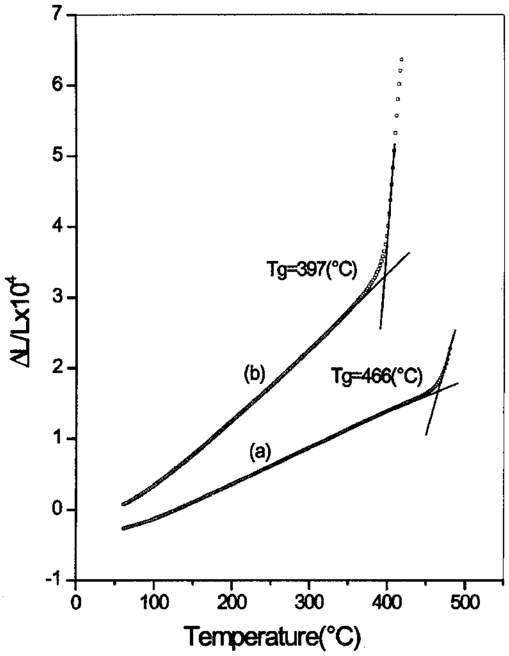

Figure 7. Variation of the linear thermal expansion as a function of temperature and estimation of the glass transition temperature for (a) $(PbO)_{0.1}(SiO_2)_{0.5}(B_2O_3)_{0.4}$ and (b) $(PbO)_{0.5}(SiO_2)_{0.1}(B_2O_3)_{0.4}$ glasses.

contrast, boron in a tetrahedral configuration is characterized by very low values of quadrupolar interaction due to small distortions, thereby giving rise to a sharp peak during MAS NMR experiments. The increase in the relative intensity of the peak corresponding to trigonally coordinated boron structural units with increase in B_2O_3 concentration above $x = 0.2$ in $(PbO)_{0.5-x}(SiO_2)_{0.5}(B_2O_3)_x$ glasses (see figures 4(c) and (d)) can be understood by considering the concentration-dependent network-forming and network-modifying behaviour of PbO. For values of $x > 0.2$, the concentration of PbO will be lower and PbO mainly acts as a network modifier; both SiO_2 and B_2O_3 compete to interact with Pb^{2+}. This will lead to an increase in BO_3-type configurations. With further decrease in PbO concentration, BO_3 structural units are forced to interact with the silicate network to form Si–O–B-type linkages.

In contrast, for $(PbO)_{0.5}(SiO_2)_{0.5-y}(B_2O_3)_y$ glasses, the relative intensities of both trigonal and tetrahedral configurations remain more or less comparable with increase in the B_2O_3 concentration; this can be attributed to the comparable extents of interaction of B_2O_3 with PbO brought about by the decreased concentration of the silicate network in the glass.

The increase in the frequency of vibration observed for the asymmetric stretching vibrations of BO_3^{3-} structural units in $(PbO)_{0.5-x}(SiO_2)_{0.5}(B_2O_3)_x$ glasses can be attributed to the conversion of ionic $B\text{–}O^- \cdots Pb^{2+}$ linkages to strongly covalent Si–O–B/B–O–B linkages in these glasses, thereby increasing the rigidity of the structure. However, such an increase is not observed when SiO_2 is replaced by B_2O_3 in $(PbO)_{0.5}(SiO_2)_{0.5-y}(B_2O_3)_y$ glasses, indicating that no Si–O–B/B–O–B-type linkages are formed in these glasses. Thus the IR studies further support the inferences drawn from ^{29}Si MAS NMR studies.

From the results presented in figures 8 and 9, it is clear that the effect of boron substitution on the values of the thermal expansion coefficient and the glass transition temperature are

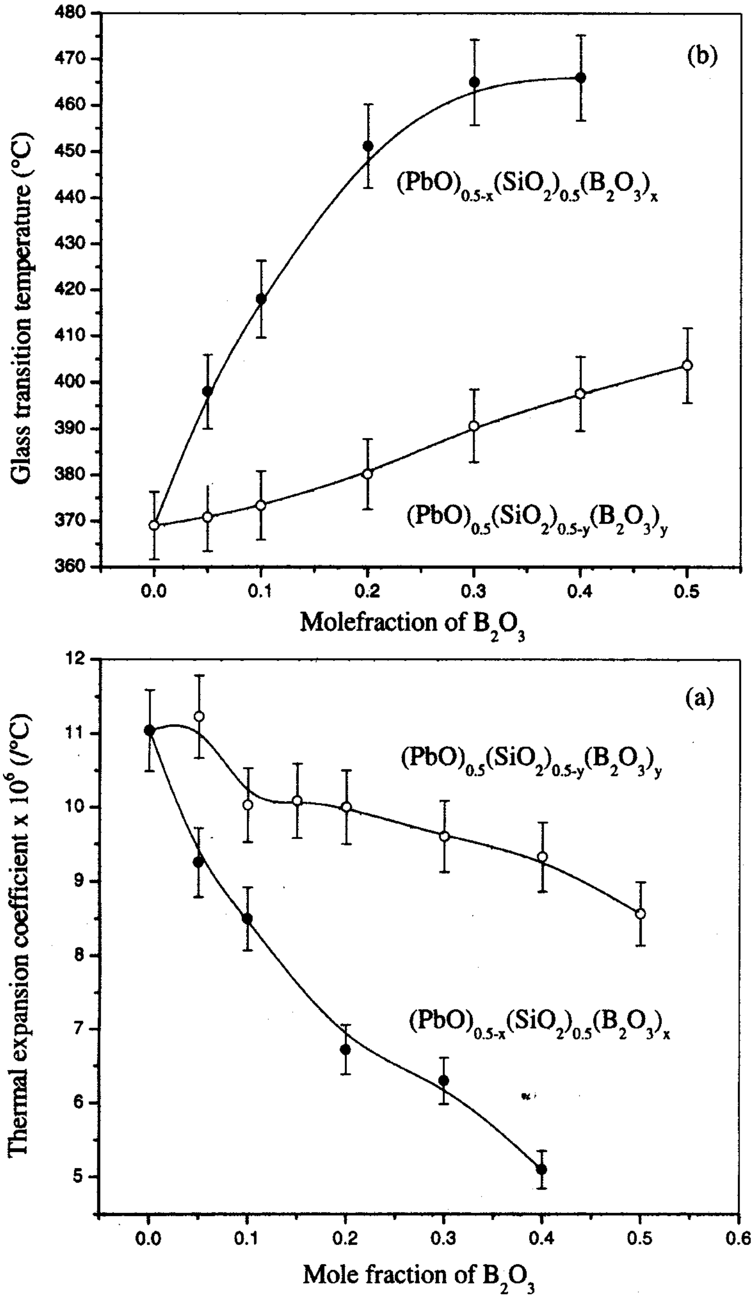

Figure 8. Values of (a) the average linear thermal expansion coefficient and (b) the glass transition temperature for $(PbO)_{0.5-x}(SiO_2)_{0.5}(B_2O_3)_x$ glasses with $0.0 \leqslant x \leqslant 0.4$ and $(PbO)_{0.5}(SiO_2)_{0.5-y}(B_2O_3)_y$ glasses with $0.0 \leqslant y \leqslant 0.5$.

more pronounced when PbO is replaced by B_2O_3. This is understandable, as the replacement of PbO by B_2O_3 leads to an increased number of Q^4 structural units and better cross-linking through the formation of covalent Si–O–B bonds, thereby leading to a more rigid structure.

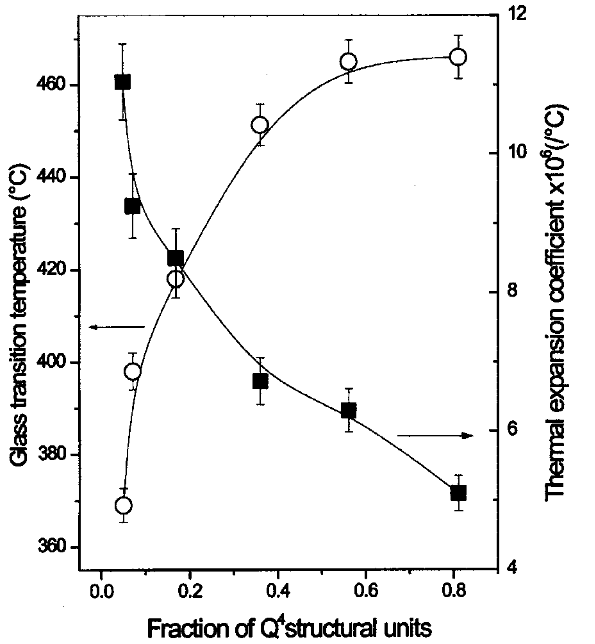

Figure 9. Variation of the average linear thermal expansion coefficient and the glass transition temperature as a function of the mole fraction of Q^4 structural units of silicon for $(PbO)_{0.5-x}(SiO_2)_{0.5}(B_2O_3)_x$ glasses with $0.0 \leqslant x \leqslant 0.4$.

The enhanced rigidity of the glass structure leads to the decrease in the thermal expansion coefficient and an increase in the values of the glass transition temperatures. In contrast, when SiO_2 is replaced by B_2O_3, the total concentration of glass-forming constituents remains the same and therefore the silicon structural configurations remain unaffected and also the relative concentration of BO_4 and BO_3 structural units remains almost constant. The slight change observed in the values of the thermal expansion coefficient and glass transition temperature for the $(PbO)_{0.5}(SiO_2)_{0.5-y}(B_2O_3)_y$ series of glasses can be understood in terms of the slightly larger B–O bond energy as compared to the Si–O bond energy, thereby leading to a slightly more rigid structure as compared to that of $(PbO)_{0.5}(SiO_2)_{0.5}$ glass. Further, the BO_4 structural units are ionically bonded to the Pb^{2+}, which may also marginally affect the values of the thermal expansion coefficient and glass transition temperatures for this series of glasses.

5. Conclusions

In conclusion, we would like to mention that, for $(PbO)_{0.5-x}(SiO_2)_{0.5}(B_2O_3)_x$ glasses with $0.0 \leqslant x \leqslant 0.4$, partial replacement of PbO by B_2O_3 results in the formation of Q^4 structural units of silicon along with Si–O–B linkages. The initial increase in the tetrahedral boron structural units and its subsequent decrease with increasing boron concentration arise due to change in the behaviour of PbO from network former to network modifier. On the other hand, for $(PbO)_{0.5}(SiO_2)_{0.5-y}(B_2O_3)_y$ glasses, when SiO_2 is replaced by B_2O_3, there is no direct interaction between SiO_2 and B_2O_3. The significant decrease in the average linear thermal expansion coefficient and increase in the glass transition temperatures for glasses having lower lead concentration have been attributed to the increased number of Si–O–B linkages and the formation of Q^4-type Si configurations which lead to enhanced rigidity in the structure of $(PbO)_{0.5-x}(SiO_2)_{0.5}(B_2O_3)_x$ glasses. The effect is less pronounced for $(PbO)_{0.5}(SiO_2)_{0.5-y}(B_2O_3)_y$ glasses.

References

[1] Tashiro H and Okuda K 1987 *J. Physique* **62** 434
[2] Anderson L P, Grusell E and Berg S 1979 *J. Phys. E: Sci. Instrum.* **12** 434
[3] Thomas G L and Sircer A 1987 *US Patent Specification* 77081 (GE Co.)
[4] Wang P W and Zhang L 1996 *J. Non-Cryst. Solids* **194** 129
[5] Bessada C, Massiot D, Coutures J, Douy A, Coutures J P and Taulelle F 1994 *J. Non-Cryst. Solids* **168** 76
[6] Fayon F, Landron C, Sakurai K, Bessada C and Massiot D 1999 *J. Non-Cryst. Solids* **243** 39
[7] Fayon F, Bessada C, Massiot D, Farnan I and Coutures J P 1998 *J. Non-Cryst. Solids* **232–4** 403
[8] Kim K S, Bray P J and Merrin S 1976 *J. Chem. Phys.* **64** 4459
[9] Bunker B C, Tallant D R, Kirkpatrick R J and Turner G L 1991 *Phys. Chem. Glasses* **31** 30
[10] Bhasin G, Bhatnagar A, Bhowmik C, Stehle M, Affatigato S, Feller J, MacKenzie and Martin S 1998 *Phys. Chem. Glasses* **39** 269
[11] Wang S and Stebbins J F 1999 *J. Am. Ceram. Soc.* **82** 1519
[12] Klyuev V P and Pevzner B Z 2000 *Phys. Chem. Glasses* **41** 380
[13] Karmakar B, Kundu P and Dwivedi R N 2000 *J. Am. Ceram. Soc.* **83/5** 1305
[14] Shrikhande V K, Sudarsan V, Kothiyal G P and Kulshreshtha S K 2002 *Proc. 13th National Symp. on Thermal Analysis* ed C G S Pillai, K L Ramkumar, P V Ravindran and V Venugopal p 213
[15] Johnson D W and Hummel F A 1968 *J. Am. Ceram. Soc.* **51** 196
[16] Dickinson J E Jr and de Jong B H W S 1988 *J. Non-Cryst. Solids* **102** 106
[17] Ross S D 1972 *Inorganic Infrared and Raman Spectra* (New York: McGraw-Hill) p 148, 260
[18] Bues W, Förster G F and Schmidt S 1996 *Z. Anorg. Allg. Chem.* **344** 148
[19] Harder U, Reich P and Willfahrt W 1995 *J. Mol. Struct.* **349** 297
[20] Dumbaugh W H and Lapp J C 1992 *J. Am. Ceram. Soc.* **75** 2315